BORON 3 (3), 139 - 144, 2018

BOR DERGİSİ
JOURNAL OF BORON
http://dergipark.gov.tr/boron

Investigation of the structural and luminescence properties of $Li_3Y_2(BO_3)_3$ synthesized by solid-state reactions

Şengül Sarıkaya Gacanoğlu[1]*, Halil Güler[2], Remziye Tülek[3], Ali Teke[4]

[1]Balıkesir University, Faculty of Science & Letters, Department of Chemistry, Balıkesir, Turkey, ORCID ID orcid.org/0000-0001-9287-8096
[2]Balıkesir University, Faculty of Science & Letters, Department of Chemistry, Balıkesir, Turkey, ORCID ID orcid.org/0000-0001-5931-829X
[3]Balıkesir University, Faculty of Science & Letters, Department of Physics, Balıkesir, Turkey, ORCID ID orcid.org/0000-0003-3988-6868
[4]Balıkesir University, Faculty of Science & Letters, Department of Physics, Balıkesir, Turkey, ORCID ID orcid.org/0000-0001-7514-762X

ARTICLE INFO

Article history:
Received 02 December 2017
Revised form 20 May 2018
Accepted 11 July 2018
Available online 30 November 2018

Research Article

DOI: 10.30728/boron.360284

Keywords:
Metal borates,
Solid-state reaction,
X-ray diffraction pattern,
Luminescence

ABSTRACT

A new binary metal borate compound, trilithiumdiyttriumorthoborate, $Li_3Y_2(BO_3)_3$ was successfully synthesized by a solid-state reaction at 1000 °C using the initial reactants of Li_2CO_3, Y_2O_3, and H_3BO_3 (molar ratio in the order; 1.5:1:3). The phase, crystallinity and size distribution of $Li_3Y_2(BO_3)_3$ was investigated by X-Ray Powder Diffraction (XRD) and Scanning Electron Microscopy (SEM). It was found that single phase $Li_3Y_2(BO_3)_3$ crystallizes in orthorhombic crystal with refined unit cell parameters of a=8.9228, b=9.5840, c=20.4469Å, Z=9 and represent the space group of Pmmm. Average particle size was calculated as 70 nm by Scherrer's equation. The luminescence properties of $Li_3Y_2(BO_3)_3$ were investigated by using steady state photoluminescence (PL) measurement as a function of temperature between 10 to 300 K. It was observed that the spectra are dominated with the transitions in the visible part of spectrum related to defects present in compound. A relatively low intensity band-to-band transition was also observed at high energy side of the spectrum centred at around 3.33 eV. This peak was decomposed into two close peaks at 3.32 and 3.35 eV using Gaussian fitting. From the temperature behaviour of peak energies of these emissions, the band gap of $Li_3Y_2(BO_3)_3$ was estimated to be 3.35 eV for the first time.

1. Introduction

Borate materials are very attractive for scientific investigations owing to their broad range of applications since they demonstrate good chemical stability, high optical quality and high transparency far in the UV region [1, 2]. Due to the myriad types of structure attainable by boron trigonal or tetrahedral coordination, many metal borates display important practices in nonlinear optical and laser applications [3]. They also have significant magnetic, catalytic, and phosphorescent properties [4, 5]. In recent years, there has been great interest in synthesis of family of the lithium borates, borosilicates and oxyborates, such as Eu^{3+} doped $Li_2B_4O_7$ [6], Cu^+ doped LiB_3O_5 [7], Sm^{3+} doped LYBO glasses [8], Dy^{3+} doped Lithium zinc borosilicate glasses [9], $LiY_6O_5(BO_3)_3$ [10], co-doped $Li_6Gd(BO_3)_3$:Tb^{3+}, Eu^{3+}, Bi^{3+} [11], Ce^{3+}doped $Li_6Ln(BO_3)_3$ (Ln =Gd, Y) [12], Eu^{3+} doped $Li_6Ln(BO_3)_3$ (Ln =Gd, Y) [13], $Li_3Ln_2(BO_3)_3$ (Ln = La, Yb) [14], $Li_3Ln_2(BO_3)_3$ (Ln=Nd, Eu, Dy and Yb) and $Li_6Ln(BO_3)_3$ (Ln=Dy and Yb) [15], $Li_3Sm_2(BO_3)_3$ [16], $K_3Y_3(BO_3)_4$ [17], $LiGd_6O_5(BO_3)_3$ [18], etc. These compounds mostly crystallize in the monoclinic space group of $P2_1/c$ with Z=4 [11].

Borates are also of interest as host lattice for luminescence ions. The photoluminescence properties of $YAl_3(BO_3)_4$ and $YAl_3(BO_3)_4$:Gd^{3+} were explained by Yoshida et al. [19]. In the former the valence band is mainly due to O (2p) state whereas the conduction band is composed of a mixed state of B (2p) and Y (4d). Yoshida et al. attributed the 7.8 eV emission peak to the transition from the O (2p) state to the mixed state of B (2p) and Y (4d). Recently, electronic band structure of $YAl_3B_4O_{12}$ has also been studied using several theoretical approaches. For example, the electronic structure and linear optical properties of $YAl_3B_4O_{12}$ were calculated by Wang et al. [20] using the density functional theory with the local density approximation. The authors concluded that $YAl_3B_4O_{12}$ has an indirect band gap of 6.54 eV and a direct band gap of 6.91 eV. The resultant total and partial densities of states (PDOS) indicate that the top valence band is composed of O (2p), B (2s), and B (2p) states and the low conduction band mostly consists of Y (4d) and B (2p) states. Dotsenko et al. [21, 22] also explained the optical absorption edge observed at higher energies of 7.3 eV in $YAl_3B_4O_{12}$. They reported that this value is comparable with those (7.1–7.2 eV) reported for other borates in which the optical absorption edge is caused by O (2p) →B (2s), (2p) transitions within the

*Corresponding author: sengulgacanoglu@gmail.com

isolated BO_3^{3-} groups. Recently, the band structures of three isotopic $LiMBO_3$ compounds (M = Mn, Fe, and Co) have been determined using first principles calculations [23]. The band gap energies for $LiMnBO_3$, $LiFeBO_3$ and $LiCoBO_3$ were calculated to be 3.15, 3.19 and 3.26 eV, respectively.

To our knowledge, neither a theoretical work on the calculation of band structure nor synthesizing and investigation of $Li_3Y_2(BO_3)_3$ were reported in the literature. In this study, an intentionally undoped $Li_3Y_2(BO_3)_3$ powders was synthesized for the first time using simple and cost effective method of solid-state reaction and investigated structurally and optically by means of XRD, FTIR and temperature dependent PL techniques.

2. Materials and methods

$Li_3Y_2(BO_3)_3$ was synthesized by high temperature solid-state reaction of a mixture of high purity Li_2CO_3, Y_2O_3 and H_3BO_3 (mole ratios in the order 1.5:1:3). The mixture was ground and preheated at 450 °C for 4 h and the sample was reground after being annealed at 1000 °C for 24 h. The sample was then cooled down to room temperature at 5 °C/minutes. The reaction was carried out by Protherm PLF 120/10 in the open air. The XRD data were collected using a PANalytical X'Pert Pro diffractometer with the CuK_α radiation (λ: 1.54059 Å, 30 mA, and 40 kV). The crystal structure was found and the cell parameters were refined by the POWD program (an interactive Powder Diffraction Data Interpretation and Indexing Program Ver. 2.2) [24]. Infrared spectrum was obtained using a Perkin Elmer 983G FTIR spectrophotometer in the 4000-400 cm^{-1} region with sample as KBr discs.

Temperature dependent photoluminescence measurements were carried out on powders placed in a close-cycled cryostat in the temperature range of 10–300 K. A frequency tripled Nd:YLFQ pulse laser at 349 nm were used for the excitation. The luminescence was collected by suitable lenses and then dispersed with a 500 mm focal length spectrometer using 1200 line/mm grating and detected by Intensified Charge Coupled Device (ICCD) camera.

3. Results and discussion

Polycrystalline samples were prepared by solid-state reaction with the following chemical reaction path:

$$3Li_2CO_3(s) + 2Y_2O_3(s) + 6H_3BO_3(s) \rightarrow 2Li_3Y_2(BO_3)_3(s) + 3CO_2(g) + 9H_2O(g) \quad \text{(Eq. A)}$$

The final products were analysed by XRD. The crystal structure of the synthesized compound of $Li_3Y_2(BO_3)_3$ was found as orthorhombic with the unit cell parameters of a=8.922, b=9.5840, c=20.446 Å and space group Pmmm by driving the POWD program [24]. The metal elements Li and Y in the synthesized product of $Li_3Y_2(BO_3)_3$ were analysed spectroscopically by ICP-OEM technique. The boron element was determined literally known Carmine method. The chemical analytical results also confirms the chemical formula of the synthesized product of $Li_3Y_2(BO_3)_3$. The density of $Li_3Y_2(BO_3)_3$ was measured with a Pycnometer using toluene as a solvent and was found as 2.66 g/cm^3. The XRD pattern of final product of $Li_3Y_2(BO_3)_3$ are given in Figure 1 and data in Table 1.

Surface morphology of $Li_3Y_2(BO_3)_3$ was also investigated by scanning electron microscope. SEM measurements were performed at Quanta FEG 200. The SEM images of $Li_3Y_2(BO_3)_3$ is shown in Figure 2. As seen, the sample consists of irregular shaped particles with various particle sizes. Small grains located on the surface of larger crystals give rise to inhomogeneous size distribution. The crystallite size of the particles were calculated by the X-ray broadening method using the Scherrer's equation:

$$D = K\lambda / \beta_{hkl} \cos\theta \quad \text{(Eq. B)}$$

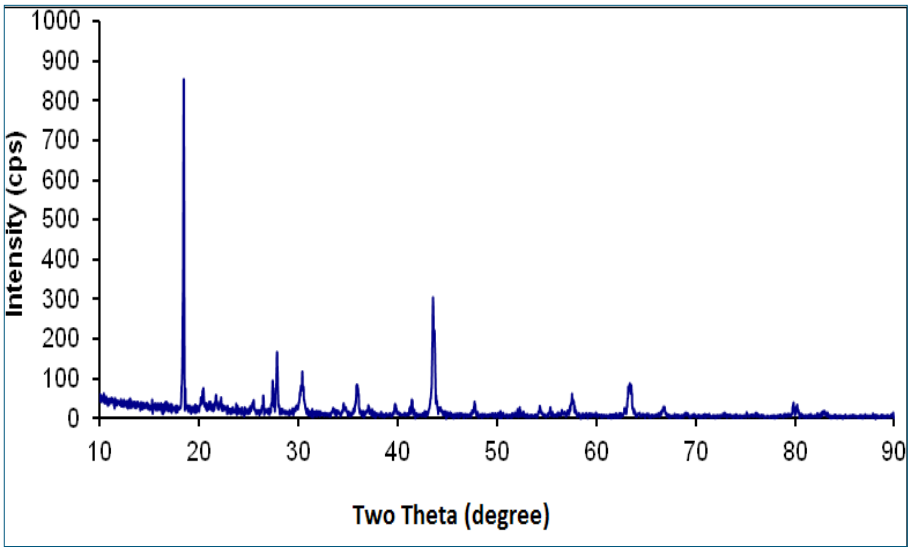

Figure 1. XRD powder pattern of $Li_3Y_2(BO_3)_3$.

Table 1. X-ray powder diffraction data of $Li_3Y_2(BO_3)_3$.

2θ degree	hkl	I/I_o Relative intensity %	$Li_3Y_2(BO_3)_3$ (Orthorhombic) Space Group: Pmmm (47)		
			$d_{calculation}$ Å	$d_{experimental}$ Å	Difference
18.4988	020	100	4.7920	4.7924	0.0004
20.4755	022	6	4.3390	4.3340	0.0050
21.7248	202	5	4.0890	4.0875	0.0015
25.5177	024	4	3.4960	3.4879	0.0081
26.5076	204	5	3.3612	3.3598	0.0014
27.4450	124	10	3.2551	3.2472	0.0079
27.9035	030	20	3.1947	3.1949	0.0002
30.4509	125	12	2.9373	2.9332	0.0041
33.5671	117	2	2.6664	2.6676	0.0012
34.5774	231	4	2.5923	2.5920	0.0003
35.9222	027	11	2.4941	2.4980	0.0039
37.1138	135	3	2.4229	2.4205	0.0024
39.7655	324	4	2.2654	2.2649	0.0005
41.4845	128	6	2.1864	2.1750	0.0124
43.5769	333	38	2.0737	2.0753	0.0016
43.7810	242	25	2.0672	2.0661	0.0011
47.8039	318	4	1.9000	1.9012	0.0012
50.6104	432	1	1.8004	1.8021	0.0017
52.3557	337	2	1.7455	1.7461	0.0006
54.3681	3 0 10	3	1.6849	1.6861	0.0012
55.4103	338	3	1.6572	1.6568	0.0004
57.6047	060	7	1.5973	1.5988	0.0015
58.2900	506	1	1.5809	1.5817	0.0008
59.0466	249	1	1.5464	1.5632	0.0168
62.9256	0 2 13	2	1.4944	1.4758	0.0186
63.2451	3 1 12	9	1.4612	1.4691	0.0007
63.5944	066	9	1.4463	1.4619	0.0156
66.8699	454	3	1.3984	1.3980	0.0004
69.0488	364	1	1.3568	1.3591	0.0024
73.065	272	0.5	1.2983	1.2940	0.0043
79.8884	3 2 15	5	1.1997	1.1998	0.0001
80.2435	706	3	1.1939	1.1954	0.0015
83.0706	558	1	1.1631	1.1617	0.0014

where D is the crystallite size, K the shape factor (0.89), λ radiation wavelength (1.5406 Å), β_{hkl} is the full width at half maximum in radian, θ is the scattering angle. Using Scherer's equation, the average particle size was calculated to be 70 nm.

The FTIR spectrum of the $Li_3Y_2(BO_3)_3$ is shown in Figure 3. The observed frequencies between 800 and 1100 cm^{-1} correspond to the stretching frequencies of tetrahedrally coordinated boron and above 1100 cm^{-1} for triangularly coordinated boron [25]. The absorption peaks below 810 cm^{-1} are also typical for triangular BO_3 groups. The bands at 1427-1147 cm^{-1} and 977-902 cm^{-1} is related to the asymmetric and symmetric stretching of B (3)–O, respectively. The bands at 723-631 and 514 cm^{-1} are the out-of-plane bending mode of B (3)–O. On the basis of these interpretations, it can be concluded that these IR bands are due to the triangular boron in the crystal structure of $Li_3Y_2(BO_3)_3$.

Figure 4 shows the evolution of PL spectra for $Li_3Y_2(BO_3)_3$ over the temperature range of 10 to 300 K. In these measurements, the laser excitation density was maintained at approx. 0.6 W/cm^2. As seen from the figure, the PL spectra were dominated by two broad peaks centred at about 2.7 and 2.0 eV at low temperature and continued to be so up to a temperature of 160 K with decreasing intensities. Above 160 K, a new peak centred at about 2.5 eV is seen to develop. The intensity of this peak increases with temperature up to 270 K and then decreases. These transitions having negligible shifts in peak energies with temperature were attributed to different types of defects present in the sample. The origin of these defects are unknown

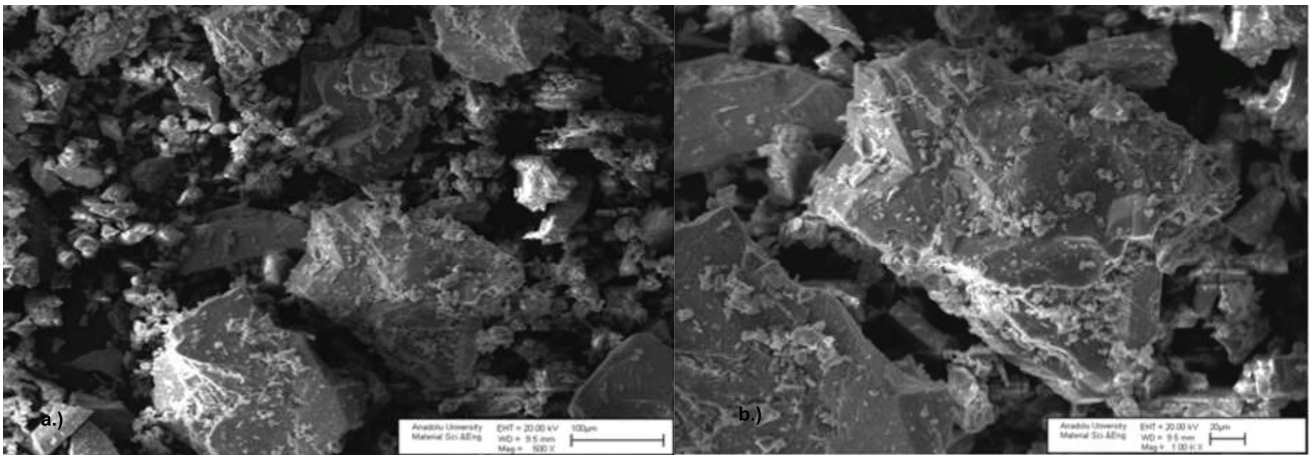

Figure 2. SEM images of the same sample of $Li_3Y_2(BO_3)_3$, a) Magnification 500 X and b) 100 000 X.

but could be related to oxygen deficiencies, intrinsic or extrinsic interstitial impurities. Since they become more dominant at different temperature regime, they could have characteristic temperature induced activation energies.

At the high-energy side of the spectra, a peak at 3.30 eV with relatively smaller intensity compared to defect related emissions were clearly observed at 10 K. By applying Gaussian fitting to this part of the spectrum, this peak was decomposed into two peaks centred at about 3.32 and 3.35 eV. The full width at half maximum (FWHM) of these peaks were deduced as 34 and 72 meV respectively. The combination of these two peaks centred at 3.33 eV can be followed up to a temperature of about 200 K. Gaussian fitting was applied to each spectrum taken at different temperatures for decomposition of this peak. The peak energy are clearly red-shifted as the temperature increases (inset of Figure 3). On contrary, no shift was observed for the defect related transitions as discussed. To identify the origin of these peaks, their temperature behaviour of peak energies were fitted by using well-known Varshni's equation;

$$E_g(T) = E_g(0) - \frac{\alpha T^2}{\beta + T} \qquad \text{(Eq. C)}$$

where $E_g(0)$ is the peak energy at 0 K obtained by interpolation and α and β are known as Varshni's thermal coefficient and Debye temperature, respectively. The $E_g(0)$, *α* and β are set as free parameters in fitting procedure. The best fitted values of $E_g(0)$ are found as 3.35 eV and 3.32 eV. The α and β values are the same for both emissions and obtained as 0.65 meVK^{-1} and 522 K, respectively. The total shifts in energies are about 35 meV for both peaks. The realization of excellent fits of Varshni's equation to the experimental results confidently indicate that these emissions could be attributed to the excitonic transitions at band-edge of $Li_3Y_2(BO_3)_3$ powder. Since neither theoretical nor experimental estimation of band gap of the studied compounds were reported so far, this finding can be considered as the first report in this sense. This assignment of the peaks can be further supported by the report on calculation of band gap of similar compounds. Seo et al. [26] estimated the band gap of $LiMnBO_3$, $LiFeBO_3$ and $LiCoBO_3$ compounds as 3.15, 3.19 and 3.26 eV, respectively using the first principle calculation. The atomic radius of Y is larger than that of Mn, Fe and Co and its electronegativity is smaller. When the stoichiometry of $Li_3Y_2(BO_3)_3$ is considered

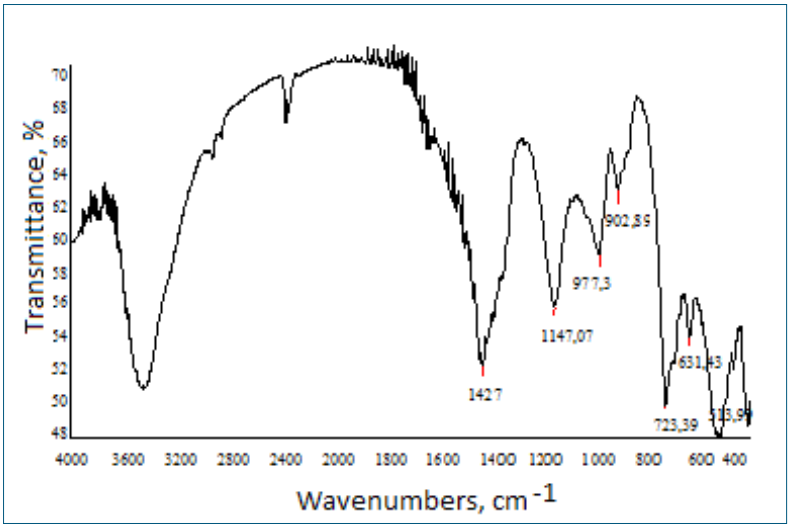

Figure 3. IR spectrum of $Li_3Y_2(BO_3)_3$ in transmission mode.

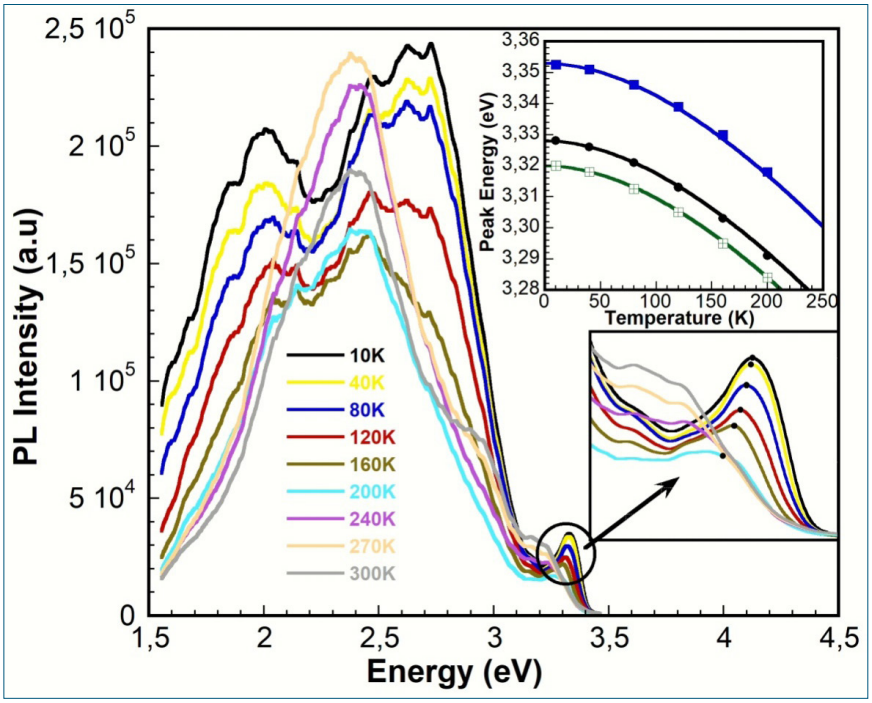

Figure 4. The temperature evolution of PL spectra for $Li_3Y_2(BO_3)_3$. One of the insets (bottom right) shows the zoom of the band edge emission region as highlighted by a circle. The other inset (top right) shows the peak positions of the band-edge emissions as a function of temperature up to 200 K, where the points deduced from experimental results by applying the Gauss fittings. The solid lines in this inset (top right) represent the fitting curves corresponding to the peak energies at 3.35 eV (blue line), at 3.32 eV (green line) and mixed at 3.33 eV (black line) using Equation C.

along with the atomic radii of Li and Y, the estimated band gap of 3.35 eV is seem to be reasonable.

4. Conclusion

The $Li_3Y_2(BO_3)_3$ compound was obtained by a solid-state chemical reaction using raw materials of Li_2CO_3, Y_2O_3, and H_3BO_3, with in the order of the mol ratio of 1.5:2:3 for the first time. The optimized synthesis reaction temperature was assigned as 1000 °C. The crystal structure of the final product was found to be orthorhombic with the unit crystal cell parameters of a=8.9228, b=9.5840 and c=20.4469 Å as determined by powder XRD technique. The number of formula units in the calculated unit cell parameter Z was calculated as 9. The space group of synthesized $Li_3Y_2(BO_3)_3$ was found as Pmmm. The surface morphology of $Li_3Y_2(BO_3)_3$ consist of irregular shaped particles. Small grains located on the surface of larger crystals give rise to inhomogeneous size distribution. Average particles size distribution was calculated as 70 nm by using Scherer's equation.

The optical properties of undoped $Li_3Y_2(BO_3)_3$ powder were studied using temperature dependent photoluminescence. The spectra were dominated by various defects related transitions along with low intensity excitonic band-to-band transitions. From the temperature behaviour of energy peak positions related to band-edge emissions, which usually fallows the band gap shrinkage, the band gap of the $Li_3Y_2(BO_3)_3$ compound was estimated to be 3.35 eV for the first time.

Acknowledgement

Authors acknowledge the support from Science & Technology Research and Application Centre of Balıkesir University.

References

[1] Keszler D. A., Borates for optical frequency conversion, Curr. Op. Solid State Mat. Sci., 1 (2), 204-211, 1996.

[2] Becker P., Borate materials in nonlinear optics, Adv. Mater., 10 (13), 979-992, 1998.

[3] Zhang Y., Liang J. K., Chen X. L., He M., Xu T., A structural study of $Ca_3La_3(BO_3)_5$, J. Alloys Compd., 327 (1), 96-99, 2001.

[4] Attfield J. P., Bell A. M. T., Rodriguez-Martinez L. M., Greneche J. M., Leblanc M., Cernik R.J., Clarke J. F., Perkins D. A., Synthesis, structure and properties of a semivalent iron oxoborate, Fe_2OBO_3, J. Mater. Chem., 9 (1), 205-209, 1999.

[5] Keszler D. A., Synthesis, crystal chemistry, and optical properties of metal borates, Curr. Op. Solid State Mat. Sci., 4 (2), 155-162, 1999.

[6] Danilyuk P. S., Puga P. P., Krasilinets V. N., Gomonai A. I., Puga G. D., Rizak V. M., Turok I. I., X-ray fluorescence of Eu^{3+} ions in glassy and polycrystalline lithium tetraborate, Glass. Phys. Chem, 44 (1), 1-6, 2018.

[7] Kananen B. E., Mc Clory J. V., Giles N. C., Halliburton L. E., Copper-doped lithium triborate (LiB_3O_5) crystals: A photoluminescence, thermo luminescence, and electron paramagnetic resonance study, J. Luminescence., 194, 700-705, 2018.

[8] Karanmam E., Kim H. J., Jayasankar C. K., Chauthima N. M., Kaewkhao J., The photoluminescence, optical and physical properties of Sm^{3+} doped lithium yttrium borate glasses, Phys. Chem. Glasses: Eur. J. Glass Sci. Technol. B, 57 (2), 85-89, 2016.

[9] Jaidass N., Krishna Moorthi C., Mohan Babu A., Reddi Babu M., Luminescence properties of Dy^{3+} doped lithium zinc borosilicate glasses for photonic applications, J. Heliyon, 4 (3), 2018.

[10] Gao J. H., Crystal structure of lithium yttrium borate $LiY_6O_5(BO_3)_3$, Chinese J. Struc. Chem., 10, 1175-1178, 2006.

[11] Chen P., Mo F., Guan A., Wang R., Wang G., Xia S., Zhou, L., Luminescence and energy transfer of the color-tunable phosphor $Li_6Gd(BO_3)_3$: Tb^{3+}/Bi^{3+},Eu^{3+}, Ap. Rad. Iso., 108, 148-153, 2016.

[12] Koroleva T. S., Kidibaev M. M., Nehari A., Pedrini C., Lebbou K., Belsky A. N., Tcherepanov A. N., Ce-doped $Li_6Ln(BO_3)_3$ (Ln= Y, Gd) Single crystals fibers grown by micro-pulling down method and luminescence properties, Opt. Mater., 35 (5), 868-874, 2013.

[13] Leskelae M., Hoelsae J., Luminescence properties of Eu^{3+} doped $Li_6Ln(BO_3)_3$ (Ln=Gd, Y) phosphors, Eur. J. Solid State Inorg. Chem., 28, 151-154, 1991.

[14] Jubera V., Crystalline structures and luminescence properties of new system compounds Li_2O-B_2O_3-Ln_2O_3, PhD Thesis, The University of Bordeaux I, France, 1992.

[15] Gamidova S. A., Triangulation in the Li_2O-Ln_2O_3-B_2O_3 (Ln= Nd, Eu, Dy, Yb, and Y) systems and the melting character of ternary compounds, Russ. J. Inorg. Chem., 54(1), 141-144, 2009.

[16] Akhmedova N. A., Guseinova S. A., Mustafaev N. M., Zargarova M. I., $Li_3Ln_2(BO_3)_3$ compound in Li_2O-Ln_2O_3-B_2O_3, Zh. Neorg. Khim., 37 (69), 1378-1383, 1992.

[17] Gao J. H., Li R. K., Preparation, structure and luminescent properties of a new potassium yttrium borate $K_3Y_3(BO_3)_4$, Mater. Res. Bull., 43 (4), 882-888, 2008.

[18] Chaminade J. P., Gravereau P., Veronique J., Fouassier C., A New Family of Lithium Rare-Earth Oxyborates, $LiLn_6O_5(BO_3)_3$ (Ln= Pr–Tm): Crystal Structure of the Gadolinium Phase $LiGd_6O_5(BO_3)_3$, J. Solid State Chem., 146 (1), 189-196, 1999.

[19] Yoshida H., Yoshimatsu R., Watanabe S., Ogasawara K., Optical transitions near the fundamental absorption edge and electronic structures of $YAl_3(BO_3)_4$: Gd^{3+}, Jpn. J. Appl. Phys. 45 (1R), 146, 2006.

[20] Wang Y., Wang L., Li H., Electronic structure and linear optical properties of $YAl_3(BO_3)_4$, J. App. Phys., 102 (1), 013711, 2007.

[21] Dotsenko V. P.,Berezovskaya I. V., Voloshinovskii A. S., Efryushina N. P., Luminescence properties of Ce^{3+} ions in magnesium fluoroborate $Mg_3BO_3F_3$, Mater. Chem. Phys., 77 (1), 141-146, 2003.

[22] Dotsenko V. P.,Berezovskaya I. V., Stryganyuk G. B., Efryushina N. P., Position of the optical absorption edge of alkaline earth borates, Opt. Mat., 31 (10), 1428-1433, 2009.

[23] Tao L., Neilson J. R., Melot B. C., McQueen T. M., Masquelier C., Gwenaelle R., Magnetic structures of $LiMBO_3$ (M = Mn, Fe, Co) lithiated transition metal borates, Inorg. Chem., 52(20), 11966-11974, 2013.

[24] Wu E., POWD, an interactive program for powder diffraction data interpretation and indexing, J. Appl. Cryst., 22(59), 506-510, 1989.

[25] Pan S., Smit J.P., Watkins B., Marvel M. R., Stern C. L., Poeppelmeier K. R., Synthesis, crystal structure and nonlinear optical properties of $Li_6CuB_4O_{10}$: A congruently melting compound with isolated $[CuB_4O_{10}]$ 6-units, J. Am. Chem. Soc., 128 (35), 11631-11634, 2006.

[26] Seo D. H., Park Y. U., Kim S. W., Park I., Shakoor R. A., Kang K., First-principles study on lithium metal borate cathodes for lithium rechargeable batteries, Phys. Rev. B, 83 (20), 205127, 2011.